International Journal of Aerospace Sciences 2013, 2(3): 124-137
DOI: 10.5923/j.aerospace.20130203.05

Design and Optimization of a Composite Vessel for Hydrogen Storage Subject to Internal Pressure and In-Flight Loads for UAVs

G. Romeo*, F. Danzi, E. Cestino, F. Borello

Department of Mechanical and Aerospace Engineering, Politecnico di Torino Corso Duca degli Abruzzi 24, 10129 Torino Italy

Abstract Research is being carried out with the aim of designinga Very-Long Endurance Solar Powered Autonomous Stratospheric UAV. This UAV could play the role of a pseudo satellite and could offer the advantage of allowing a more detailed land vision due to its relative closeness to land (17-20 km) at a much lower cost than a real satellite. Two different configurationsare under investigation in order to decide on the best solution that will completely satisfy the a priori imposed constraints. In recent years, the aeronautical community has increasingly focused on the design of solar powered platforms and zero emission airplanes; a coupled system (solar array and hydrogen fuel cells) can be used to supply energy throughout the entire day in order to ensure the continuous flight for several months. As known, a fuel cell system requires at least a couple of external tanks for fuel storage. Hydrogen and oxygen are stored using a pressure vessel installed inside the wing. In this way, the stored gases are subjected not only to pressure loads but also to in-flight loads that can abruptly change the optimum layout required to satisfy regulation requirements. A parametric analysis has been performed to define the optimum layout and the number of tanks necessary to supply the required power. In addition a genetic algorithm has been used to optimize the laminate layup in order to reduce the weight of the tank and ensure that it can resist without at failing catastrophically.

Keywords FuelCell, Hydrogen Storage System, Pressure Vessel, Solar HALE-UAV, Optimization, Genetic Algorithm

1. Introduction

UAV technology has advanced to such an extent that the aeronautical industry is now ready to expand into a new ‘added value’ Commercial industry. UAVs could be used in many applications ranging from border and costal patrol to homeland security, maritime surveillance, forest fire mapping, volcano eruption and many more. One of the great advantages of UAVs and, consequentially one of the most important reasons for their success, is the wide variety of operative characteristics of the vehicles; each mission can therefore be performed with a specifically designed machine. UAV related technology has reached a high level of maturity for some tasks, while other tasks that could be achieved by UAVs are far from being feasible because of the inherent complexity of the vehicles that could be deployed forthese purposes. These kinds of UAVs are still the subject of different research programmes.

Research is currently being carried out,under the coordination of the first author,with the aim of designing a Very-Long Endurance Solar Powered Autonomous Stratospheric UAV (VESPAS-UAV)[1-11]; two different configurations (Fig. 1, Table 1) have been developed during the research programme.

Table 1. The main characteristicsof the HeliPlat and Shampo UAVs

Description	Symbol	Value HELIPLAT	Value SHAMPO
Flight Altitude	Z	17000 m	17000 m
Max. power available for the payload	P_{PL}	1000 W	1300 W
Avionic mass	W_{AV}	25 kg	32 kg
Max payload mass	W_{PL}	100 kg	100 kg
Structural mass	W_{STR}	345 kg	430 kg
Solar cell mass	W_{SC}	78 kg	127 kg
Take-off weight	W_{TO}	840 kg	924 kg
Power available for the avionic	P_{AV}	300 W	325 W
Cruise Flight power supplied to the electric motors	P_{FLY}	7300W	6700W
Efficiency energy storage system	η_{PC}	0.6	0.6
Density energy storage system	W_{FC}	600 Wh/kg	550 Wh/kg
Efficiency solar cells	η_{SC}	0.21	0.21
Efficiency electric motors	η_{M}	0.95	0.95
Efficiency propeller	η_{prop}	0.85	0.85
Number of motors	N	8	8
Cruise airspeed (TAS)	TAS	20 m/s	25 m/s
Wing span	b_W	73 m	73 m
Wing surface	S_W	176.5 m^2	192 m^2
Aspect ratio	AR_W	30	28
Root chord	c_{root}	2.97 m	9 m
Tip chord	c_{tip}	0.95 m	0.9 m
Sweep angle	Λ_W	0 deg	5 deg

* Corresponding author:
giulio.romeo@polito.it (G. Romeo)
Published online at http://journal.sapub.org/aerospace

No real very-long endurance stratospheric platform is currently available in Europe, while only afew are available in the USA. A solar-powered unmanned aircraft is at present being developed by Boeing and QinetiQ for the US Government for use in military and civil tasks.

This type of vehicle could play the role of a pseudo satellite and offer two main advantages: first, it guarantees a higher observation resolution, due to its relative closeness to land (17-20 km) and second, it could be employed at a lower cost than the satellites currently in use. The greatest constrain for missions of such an UAV is the very long endurance (4-6 months to several years) that is required to guarantee continuity in data transmission that a satellite should provide; one way of obtaining very long endurance is to provide the platform with an almost closed cycle power system.

The solution considered for the research reported in[1-11] is a power system that exploits solar energy during the day (to supply the UAV and produce oxygen and hydrogen through the use of an electrolyser) and a fuel cell system during the night (fed by the hydrogen and oxygen stored during the day phase). This closed-loop system generates the power during the daytime from thin, high efficiency solar cells that cover the aircraft's wing and horizontal tail.These cells supply power to the electric motors for flight and to an electrolyser, which splits water into its two components, hydrogen and oxygen. The gases are stored in pressurized tanks (80-350 bar) and then, during the night, are used as inlet gases for the fuel cell stack in order to produce electric DC power and water which is supplied to the electrolyser. Since the fuel cells guarantee clean and efficient power generation, they can be considered a suitable alternative to conventional energy sources[12].

The storage of the gases in such a configuration plays an important role in ensuring an improvement in endurance since the tanks need to work at very high-pressures and be as light as possible in order to minimize the power required for flight.

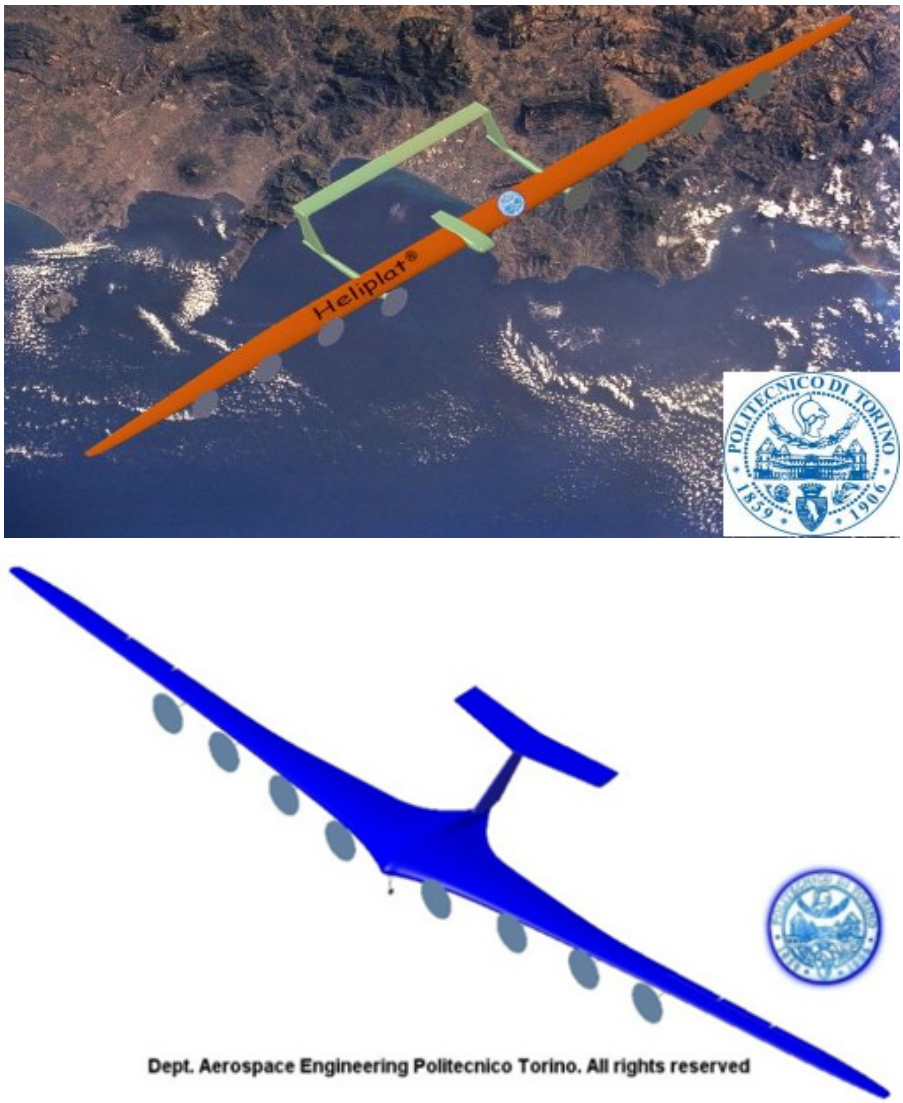

a)

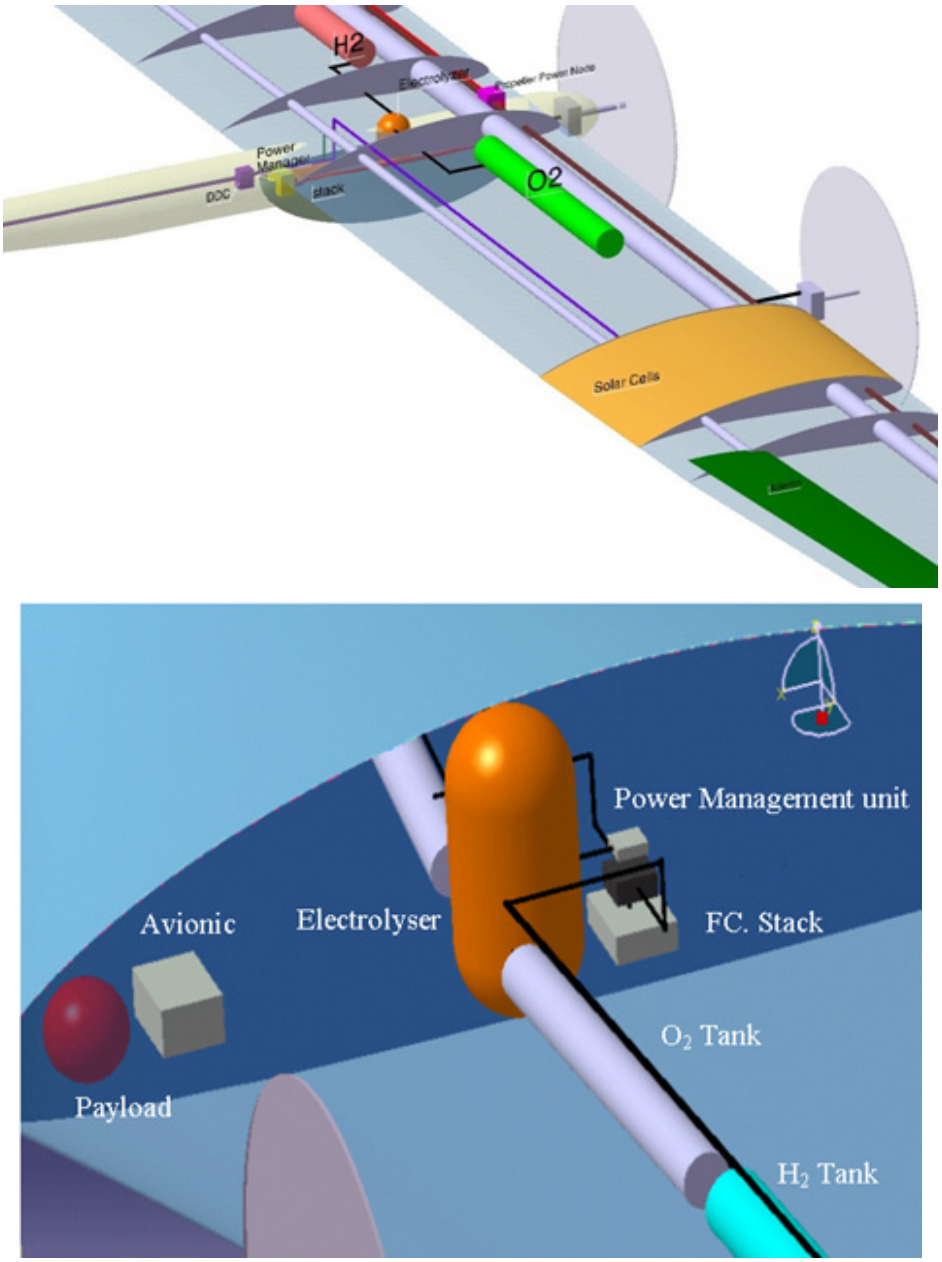

b)

Figure 1. a) The HeliPlat and the Shampo High Altitude Long Endurance Solar powered POLITO UAVs, b) 3D CAD model of the preliminary internal layout of both configurations

The characteristics of HeliPlat (**Heli**os **Plat**form) and Shampo (**S**olar **H**ale **A**ircraft **M**ulti **P**ayload & **O**peration), which are shown in table 1, highlight the main differences in the two configurations. Less internal space is available in the HeliPlat configuration and this means the tank diameter must be two or three times smaller than the Shampo tank diameter. Therequired tank volume is approximately the same for both configurations, as the required flight power is approximately the same. This implies that a longer tank is required for the HeliPlat configuration. As a consequence the effects of inertial loads are more severe for the HeliPlat configuration and this explains why a diameter of 0.31 m has been considered for the analysis. A 3D CAD model of the preliminary internal layout has been set upfor both configurations using CATIA V5. Fig. 1b shows a possible installation of the FC system and tanks in the HeliPlat and Shampo configurations.

The choice of installing the tanks inside the wing was mainly dictated by the added relief loads caused by the weight of the tanks; a higher aerodynamics drag has also been considered in the case of external pods (below the wing). The decision to install the tanks inside the wing, in the case of the HeliPlat configuration, was also dictated by the fact that the limited volume of the fuselage is already occupied by the payload bay.

Furthermore, as shown in[21], the presence of large external pods mounted ontoan airplane wing can also significantly influence the aeroelastic properties of the wing;

a reduction in flutter speed was obtained when a tip pod was included in the aeroelastic analysis of typical HALE wings[21]. Several investigations on the mishap of Helios UA Vhave confirmed that wing failure occurred due to the presence of an external fuel tank at the wing tip (with the tank almost empty at the time of the failure). It has been suggested that flutter occurred because of the unusually low speed that resulted due to the presence of the pod[22]. A FEM aeroelastic analysis of the Shampo configuration, which is reported in reference[23], showed that no critical speeds had been detected up to 100 m/s. It is possible to conclude that the proposed configuration satisfies the airworthiness target as far as the design diving speed is concerned.

Different tools have been developed to optimize the stacking sequence of composite pressure vessels subjectedto inertial loads and to ensure that the regulation requirements concerning burst pressure are met.

The optimization of the tank, which has been designed with and without inertial loads, for the HALE configurations developed by the authors, is presented in this work.

2. General Sizing of the Hydrogen Tanks

The operational conditions of the tanks need to be evaluated taking into account some general constraints; since the tanks are positioned inside the wing, the main geometrical constraints are set on the basis of the wing profile (the external diameter must be less than the thickness of the wing) and feasibility (the length of the tank should not exceed 4 meters due to technological and manufacturing aspects). This constraint is particularly relevant for the HeliPlat configuration where the maximum wing thickness is 0.32m. Another important constraint concerns the electrolyser system; the optimal operational condition for this system is in fact the one in which hydrogen and oxygen are produced at a pressure of 100 bar. A pressure of 100 bar pressure was chosen as the operative pressure of the tanksin order to avoid additional equipment for weight, safety and reliability purposes.

Only the internal pressure was considered for the general sizing. The inertial loads and loads due to bending and torsion of the wing were neglected. If these constraints are taken onto account, the mass of gas that needs to be stored has to be considered in order to define the overall dimensions of the tank. The hydrogen tank was chosen as the reference study casein this work; the oxygen tank (required in HALE applications because of the flight altitude) can be sized and analysed in a similar way.

An estimate of the hydrogen mass requirement to supply power for night flight can be determinedthrough the following basic analysis, as in[13]. The voltage of an individual cell in a PEM fuel cell stack is given by:

$$V = 1.2\,\eta_{FC} \tag{1}$$

where V is the cell voltage and η_{FC} is the electrical conversion efficiency of the cell. The flow rate of hydrogen (F_H) [Kg/s] required to produce the output power, for a given desired output power P_O, is:

$$F_H = P_O/(1.158E8\,\eta_{FC}) \tag{2}$$

and finally, the total requiredmass of hydrogen is based on the operational time [hours] of the fuel cell:

$$M_H = F_H\,t \tag{3}$$

The data used forthe present analysis are shown in Table 2.

Table 2. FC reference operational data

Variable	U.M.	Value
Power required	W	9000
Current density	A/m^2	100
Cell Tension	V	0.816
Operational time	hours	12
Hydrogen flow rate	Kg/s	0.000114
Hydrogen mass	Kg	4.938287

Once the mass is known and assuming that hydrogen has similarbehaviour to an ideal gas, it is possible to establish the relationship between the internal pressure and the required volume, as can be seen in the hyperbole shown in Figure 2.

The location of the pressure vessel inside the wing is another important point; it is necessary to consider that the curvature of the wing induces an additional bending moment of the tank. In order to reduce the effect of the bending moment of the wing, the tank should be placed as near as possible to the wing root where the curvature induced by thebending moment of the wing is at its lowest. A mechanical system that will allow displacements of the tank along the wing span is at present under study. It hasalso been considered appropriate to place the tank as close as possible to the shear centrein order to minimize the effect of torsional loads.

As previously mentioned a pressure of 100 bar was chosen; besides the necessity of additional compressors to increase the storage pressure from 100 bar (electrolyser output) to higher values, there are other reasons for this choice. A higher storage pressure wouldlead to a smallertank but would also imply an increase in weight of the tank. It can be seen, from Figure 3, that thisincrease in weight is linear with the pressure increment (under the assumption of a qualitative thin wall analysis[15]) since the wall thickness is basically linear with the ultimate load (burst pressure). Moreover, an increment in tank weight is usually connected to an increment in the weight of the equipment, e.g. the operational valves, safety valves, and the pipeline need to be sized for a higher pressure.

As a pressure of 100 bar was chosen,two tanks are required to store the whole massfor the assigned operational condition. The volume computed considering the chosen tank geometry is slightly greater than the theoretical one asa small reserve of hydrogen has been added to be used in the case of an emergency or to contrast a higher wind jet-stream.

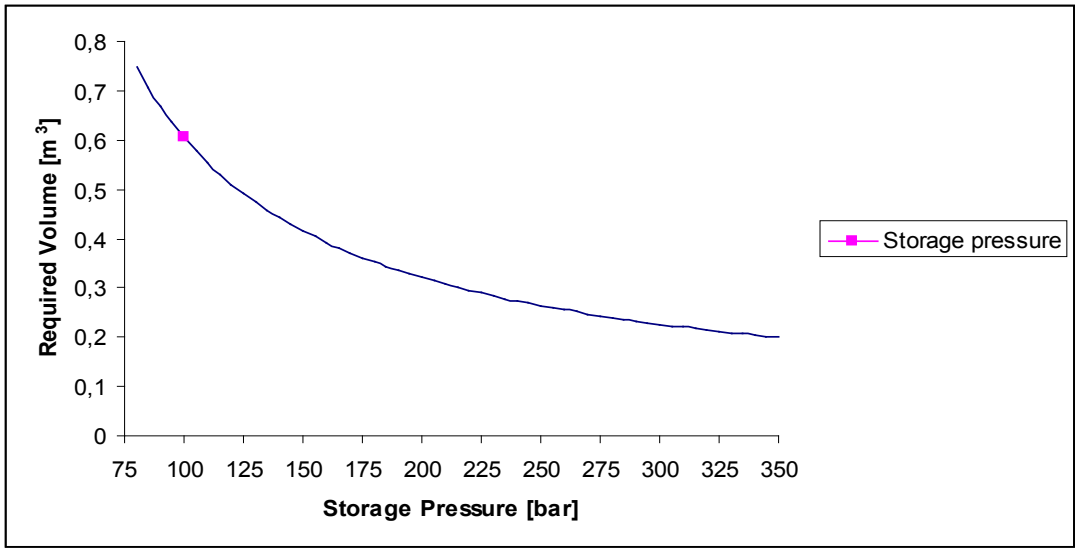

Figure 2. Tank Volume vs.storage pressure

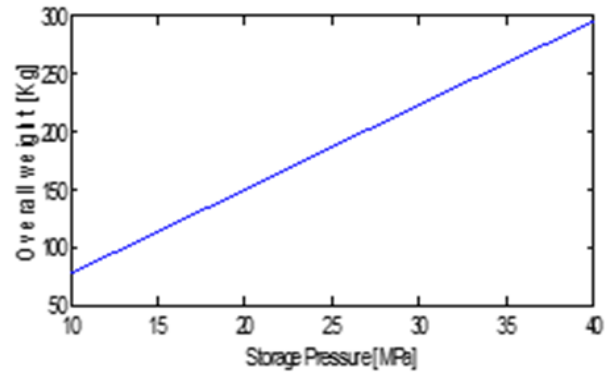

a)

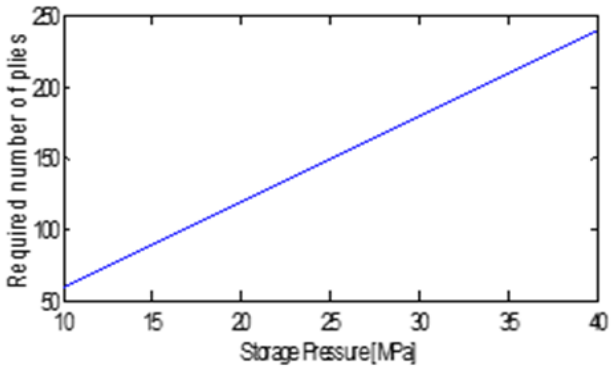

b)

Figure 3. a)Number of ply and b) overall weight variation vs storage pressure

3. Progressive Ply Failure Analysis

The burst pressure of the pressure vessel was evaluated in reference[14] by computing the first ply failure (FPF)of the laminate, while Tsai[15] suggested that the burst pressure should correspond to the last ply failure(LPF). However the FPF and LPF are coincident for the stacking of the same-orientationangle-ply laminate subjected to membrane loads. The layup obtained in this work shows a non-constant distribution of orientations, because inertial loads are taken into account and the laminate FPF and LPF could therefore be different. Both burst pressures definitionshave been compared in the present analysis.

A Matlab® programme has been developedto carry outthe Progressive Ply FailureAnalysis. The Tsai Hill criterion[13] was chosen as the failure criterion. In the developed code, if a generic ply fails under the considered loads, the stiffness matrix is updated considering a degradation factor of zero, i.e. the lamina contribution to stiffness is neglected, regardless of the failure mode.

The deformation induced by the previous loads has been taken into account in order to restore linearity between the applied loads and the failure index. The code continues iteratively until LPF is reached. A block diagram of the developed tool is shown in Figure 4. A series of composite laminates has been studied to validate the PPFA code and the results have been compared with both experimental and FE results.

A composite laminate of T300/5208 graphite-epoxy with 24 layers andan S (S=a/h) of 150 was considered in Ref.[16]. The studied layuphas the following configuration: $[\theta_4/0_4/-\theta_4]_s$. The laminate was subjected to uniaxial load N_x. The FE results in Ref.[16] were compared with Soni's experimental data[17].

The same set of laminates has also been studied with MSC Patran®/Nastran® using QUAD4 elements. The results obtained in[16],[17] and fromPatran®/Nastran® have been compared with the results obtained from the PPFA code.The value of tension shown in Figure 5 is a tension mean value which has been evaluated as follows:

$$\sigma_m = \frac{FL}{h} \tag{4}$$

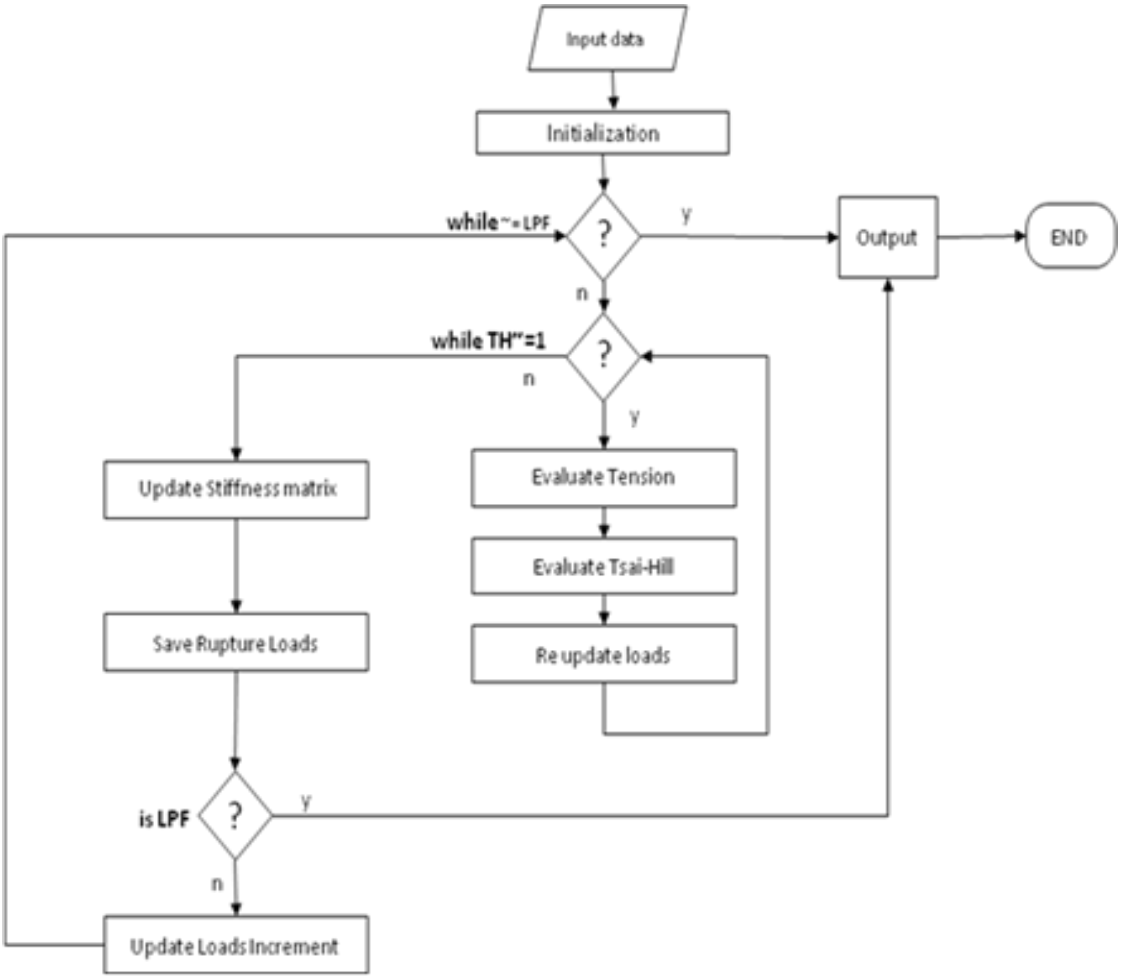

Figure 4. PPFA block diagram

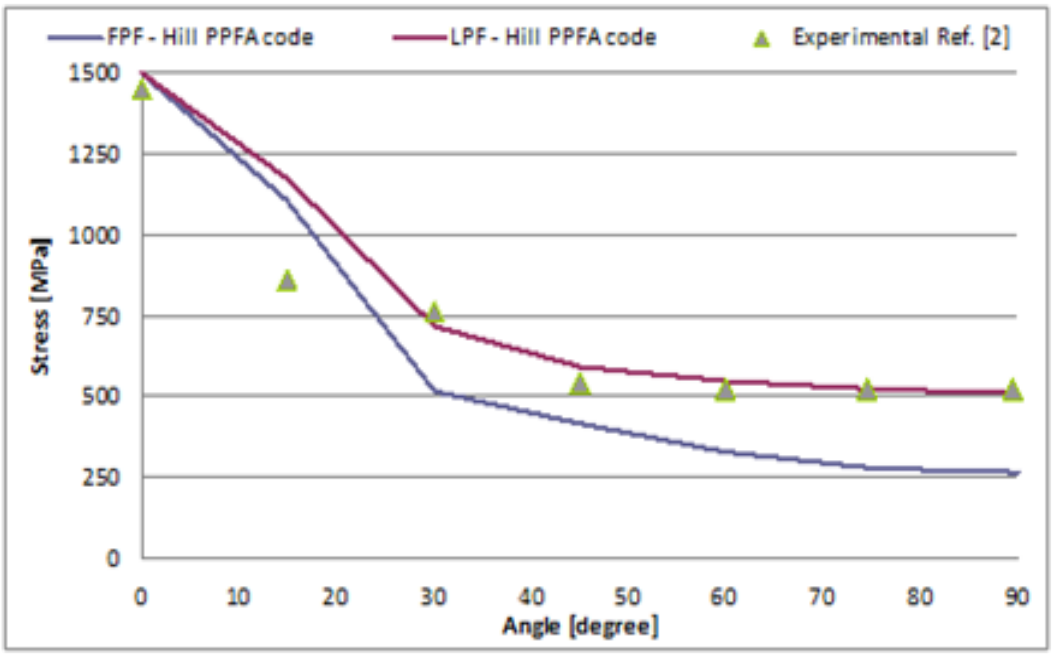

(a)

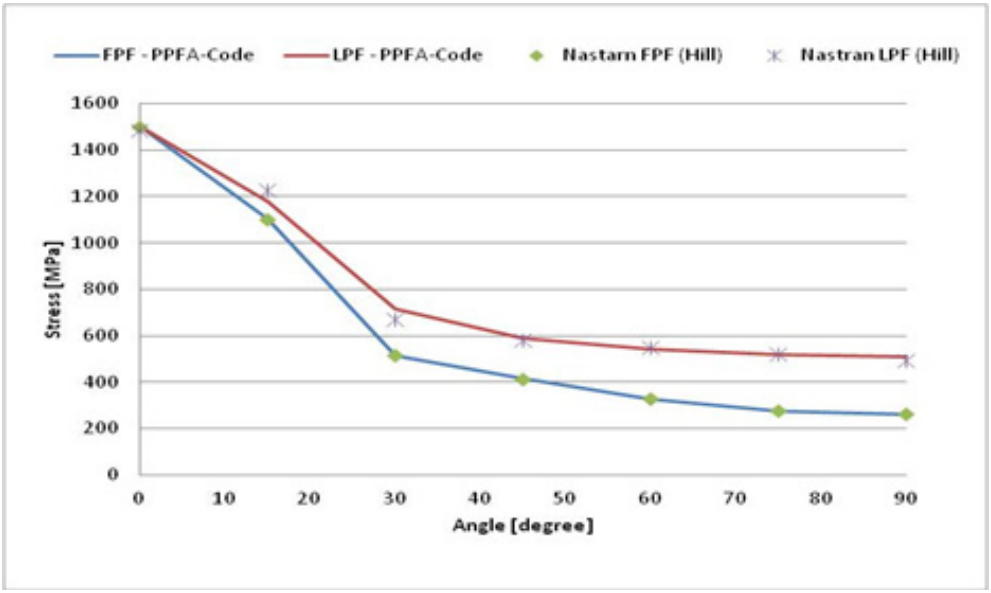
FPF - PPFA-Code
LPF - PPFA-Code
Nastarn FPF (Hill)
Nastran LPF (Hill)
Stress [MPa]
Angle [degree]

(b)

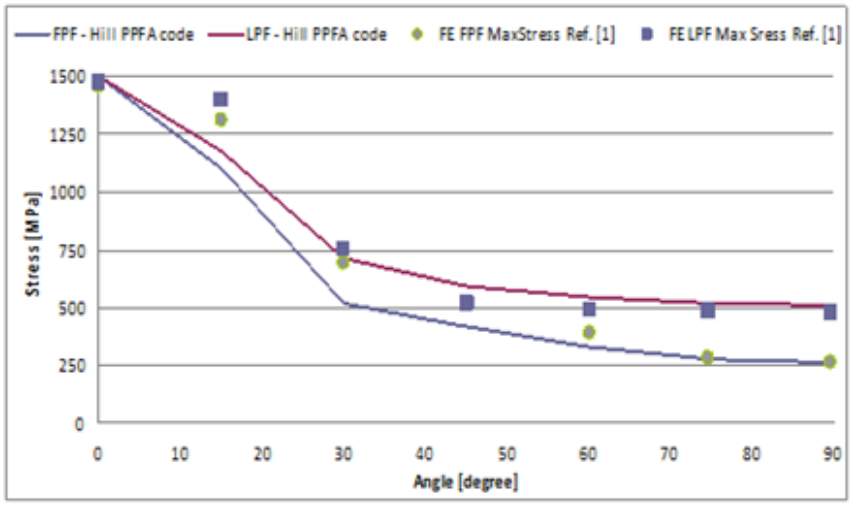
FPF - Hill PPFA code
LPF - Hill PPFA code
FE FPF MaxStress Ref. [1]
FE LPF Max Sress Ref. [1]
Stress [MPa]
Angle [degree]

(c)

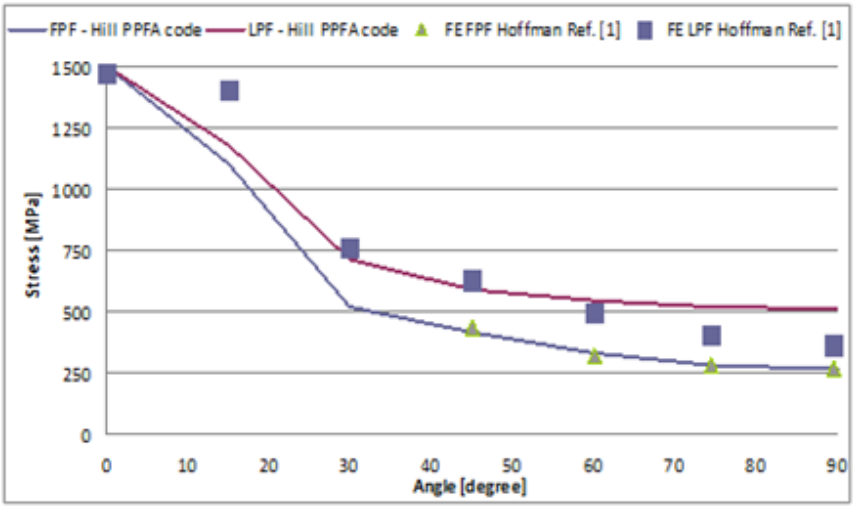
FPF - Hill PPFA code
LPF - Hill PPFA code
FE FPF Hoffman Ref. [1]
FE LPF Hoffman Ref. [1]
Stress [MPa]
Angle [degree]

(d)

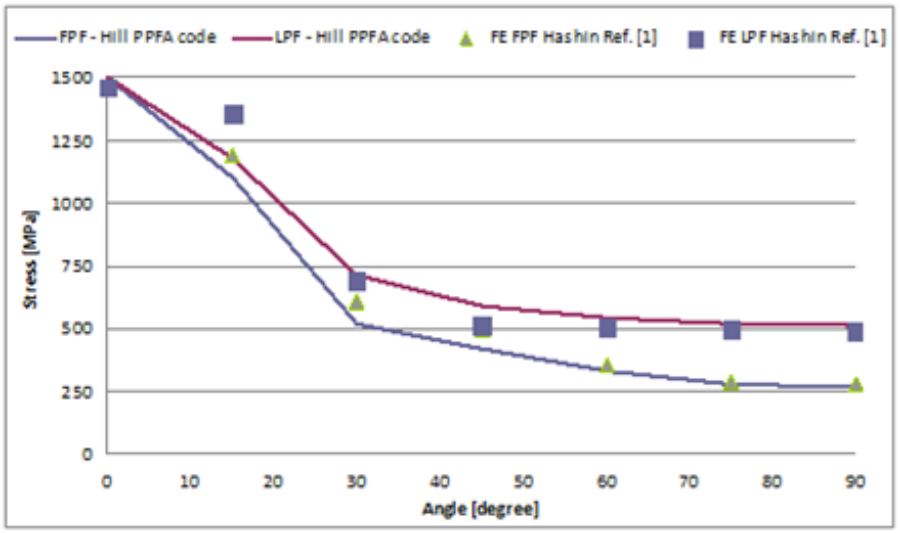

(e)

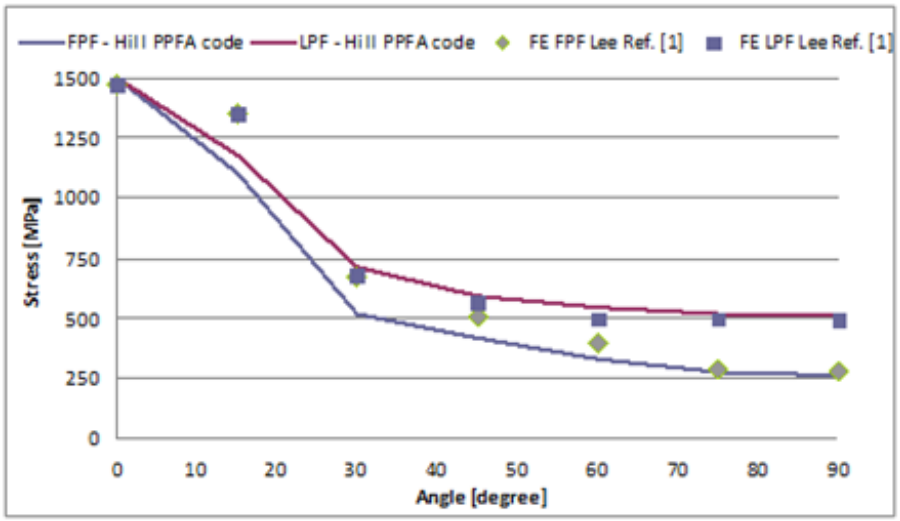

(f)

Figure 5. Comparison of the stress results

Table 3. FPF and LPF Load per unit length [N/mm] predicted with the PPFA code for the $[\theta_4/0_4/-\theta_4]_s$ laminate

θ	FPF Load	LPF Load
0	5400,00	5400,00
15	3966,49	4235,34
30	1854,87	2566,65
45	1494,17	2119,79
60	1178,64	1957,82
75	993,23	1873,19
90	944,66	1841,06

The experimental results fall close to the failure curves, with the exception of the 15° point, which is considerably lower than the predicted values. Soni[17] stated that the failure mechanism of the 15° specimen was due to extensive delaminations at the free edges, followed by tensile fibre failure. It should be noticed that the current analysis has neglected both delaminations and free edge effects.

The difference between FPF and LPF for laminates with lower orientations than 30° is somewhat small, as expected. This is due to the fact that, for these angles, the fibres run primarily in the direction of the applied load. The first failure in each case was due to fibre failure of the θ°/-θ° laminae. A good correlation has been achieved between the experimental results and the predicted failure loads with the PPFA Matlab® code.

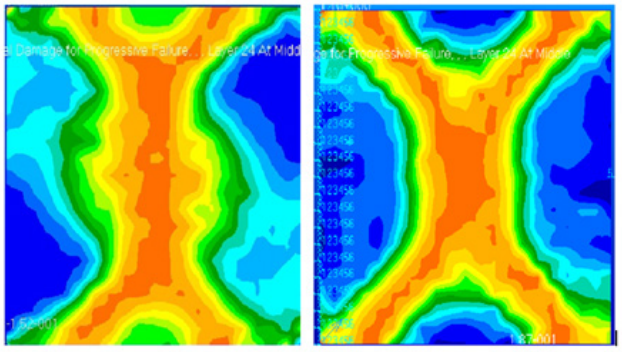

Figure 6. Nastran SOL400 Fully Damaged panel a) the 30° case b) the 45° case

The PPFA code shows very good behaviour, in comparison to the Nastran nonlinear progressive failure analysis (SOL 400), as can be seen in figure 5f. The Nastran nonlinear progressive failure analysis damage results are reported in figure 6, for the fully damaged step, for the two configurations (30° & 45°); the orange colour indicates the zone in which the maximum value of the total damage has been reached and where continuity of the structure has been lost above the LPF.

The failure analysis of the composite laminates is complex due to the fact that geometric non-linearities cannot be neglected when the loads are increased beyond the first ply failure; this is due to the large displacements that arise after first ply failure and before the ultimate failure. in this particular example, the load is applied by enforced displacement at the free end of the laminate and by gradually increasing the displacement and monitoring the constraint forces.

The LPF can be evaluated by plotting the translational constraint force as a function of the displacement and evaluating the obtained maximum load point.

4. Genetic Algorithm

A GA[24] has been first developed to optimize the layup of a laminate subject to given mechanical, thermal and hygroscopic loads. The GA core is the MacroMec code, which was developed by the authors, using Matlab®, to evaluate stresses and strains in a given composite laminate. A block diagram of the GA is shown in Figure 7.

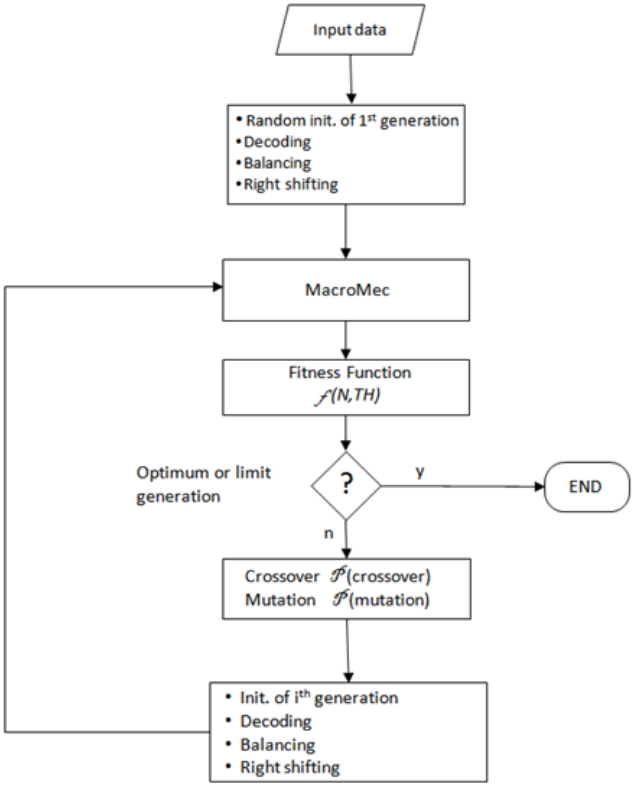

Figure 7. Genetic Algorithm block diagram

The objective of the optimization is to determine the minimum weight of laminates and the best ply orientation in order to ensure the required resistance to the applied loads without failure. The thickness of the laminae is fixed at 0.15 mm and the chosen material is T300/5208 graphite-epoxy. The chosen failure criterion is the Tsai – Hill criterion. Thus, the fitness function is a function of the Tsai – Hill index and the number of plies. The fitness value is enforced to zero if a given laminate has a greater or equal Tsai-Hill index to one.

The allowable orientation set is fixed; in other words, the orientation is a discrete subspace of the possible orientations.

The probability of mutation is fixed at 0.3. Three kinds of genetic modification are considered (swap, deletion and mutation). Each kind of genetic modification is associated with an integer; the kind of modification that is used depends on a random generated number with a uniform distribution. The *mutation* function randomly changes a gene of a given laminate; the *deletion* function deletes a gene from the layup, and the removed gene is selected randomly. The *swap* function changes in the position of two genes in the chromosome. Two termination criteria are chosen. The first one pertains to the convergence of the population while the second one is related to the number of iterations in which the optimum layup does not change. A penalty function has also been written to penalize any layup with excessive deformation.

Since, at this step, the optimization of a given panel is independent of the others, parallel computing has been used in order to reduce the computational time.

The *coupling* function assigns the number of allowable couplings to each laminate. Since the number of couplings is proportional to the fitness function of each laminate, rounded to the nearest integer, the number of total couplings may, in some cases, exceed half of the population. This means that the (i+1)th generation may have a larger dimension than the previous ones. In this case, the algorithm inhibits the creation of sons of the laminates that have a lower fitness.

The *marriage* function randomly selects which laminates will be coupled, while the *singlecop* function choses a cross-over-point according to the minimum length of the encoded laminate. Elitism is also permitted in order to ensure a fixed dimension of the population.

The GA runs until optimum has been reached, according to the above mentioned criteria, or until the limit number of generations has been generated.

5. Pressure Vessel Optimization

The Pressure vessel (PV) optimization scheme is shown in Figure 8. Given a laminate layup, the algorithm computes the weight of the tank as the sum of the liner mass, ply mass, hydrogen mass and accessory package. The latter contribution, as indicated in[12], was estimated as 50% of the tank mass while the linear mass was evaluated as 10% of the tank mass. The inertial loads were evaluated by multiplying the whole mass by the ultimate load factor.

From a technological point of view, since the vessel will be realized by tape winding, the laminate sequence must be the same for the whole tank and the design bending moment should be the maximum bending moment reached at the centreline.

Furthermore, if the pressure vessel is considered as a pinned-pinned beam, the bending moment induces a membrane load:

$$N_{\bar{x}\bar{i}} = \sigma_i s_i$$

where σ was obtained using Hooke's law, ε being known

$$\varepsilon = -\frac{M_z(EJ_x) + M_x(EJ_{xz})}{(EJ_x)(EJ_z) - (EJ_{xz})^2}x + \frac{M_x(EJ_z) + M_z(EJ_{xz})}{(EJ_x)(EJ_z) - (EJ_{xz})^2}z$$

and where

$$E_i = \frac{1}{s_i}\left(A_{11} - \frac{{A_{11}}^2}{A_{22}}\right)_i$$

Once the inertial loads have been computed, the algorithm compares them with the inertial loads evaluated in the previous iteration. If they are different, the procedure first adds pressure loads and the genetic algorithm optimizes the layup with the new updated loads. Vice versa, if they are equal, the laminate layup cannot be improved and the algorithm updates the last computed strains given as the GA output. At this step, these strains are used to compute the corresponding state of stresses; these stresses, together with the PPFA code, are used to evaluate the safety margin of the tank. The PPFA, in fact, provides an evaluation of the ultimate load (FPF or LPF) and the pressure-generated stresses.

The safety margin can be expressed in the PPFA, in terms of the difference between the applied pressure and the burst pressure (considering that the inertia-generated stresses are assumed as the starting stress status of the tank):

$$p_{burst} = p_{ex} + \Delta p \tag{5}$$

where:

$$\Delta p = \frac{4\,\Delta N_{x\ FPF,LPF}}{D} \tag{6.1}$$

or equivalently:

$$\Delta \mathrm{p} = \frac{2\,\Delta \mathrm{N}_{\mathrm{y\ FPF,LPF}}}{\mathrm{D}} \tag{6.2}$$

Let us assume that only pressure loads act on the tank. The optimum layup for angle ply laminate, as computed by the GA, is $[+53.5°/-53.5°]_{12S}$, as shown in Figure 9; the failure index shows a minimum for an orientation of 53.5°, which means that the safety margin is at a maximum. Furthermore, the Tsai-Hill index exceeds one, for ply orientations of less than 44.5° or of more than 62.25°, and this means that a laminate is unable to resist the applied load. The burst pressure for $[+53.5°/-53.5°]_{12S}$ is 201.6 bar. The FPF and LPF loads are coincident for this angle-ply laminate case, and the computed burst pressure is therefore the same for both cases.

The effect of inertial loads, may change the laminate layup that is needed to ensure conformity with the chosen failure criterion. A remarkable difference in the lay-ups, was noted in the present analysis with and without inertial loads. The bending moment (M_x) causes the PV to require an improved stiffness along the longitudinal axis of the tank and this is confirmed by the changes in the laminate lay-up. A 0° filament orientation was excluded from the subspace of possible orientations in the genetic algorithm, since this filament-wound is technologically difficult to obtain. The minimum allowable angle is 5°. The optimized layup provided by the GA runs is:

$[(+5/-5)_8\ (+53.5/-53.5)_2\ (53.5)\ (90)_2$
$(-53.5)\ (90)_2\ (+53.5)\ (90)_2\ -(53.5)]_S$

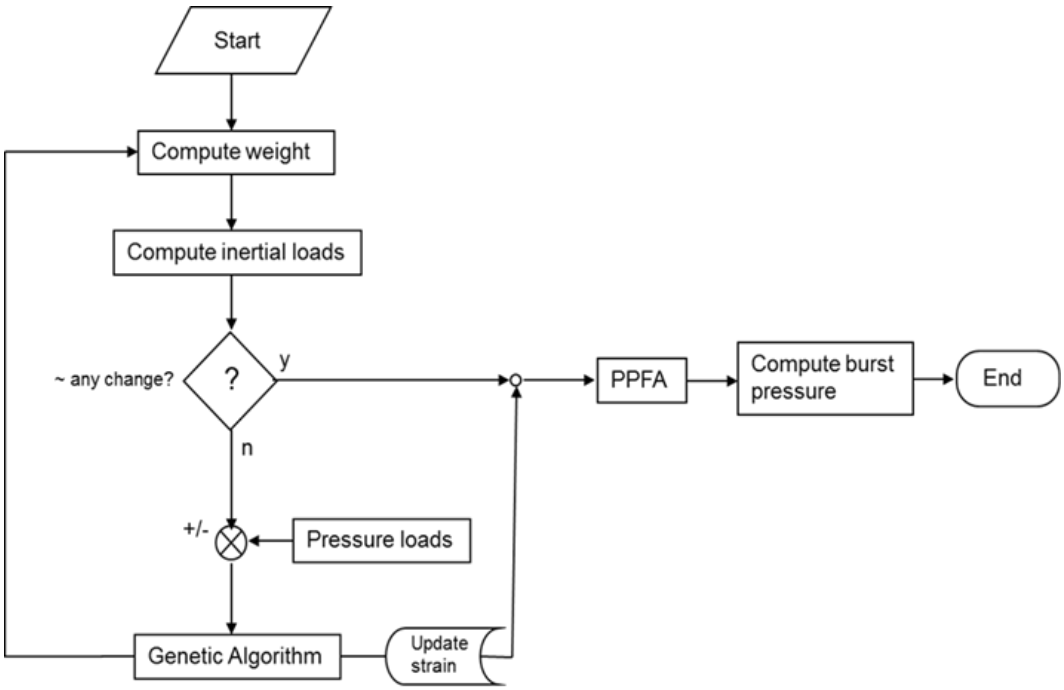

Figure 8. Pressure vessel Optimization scheme

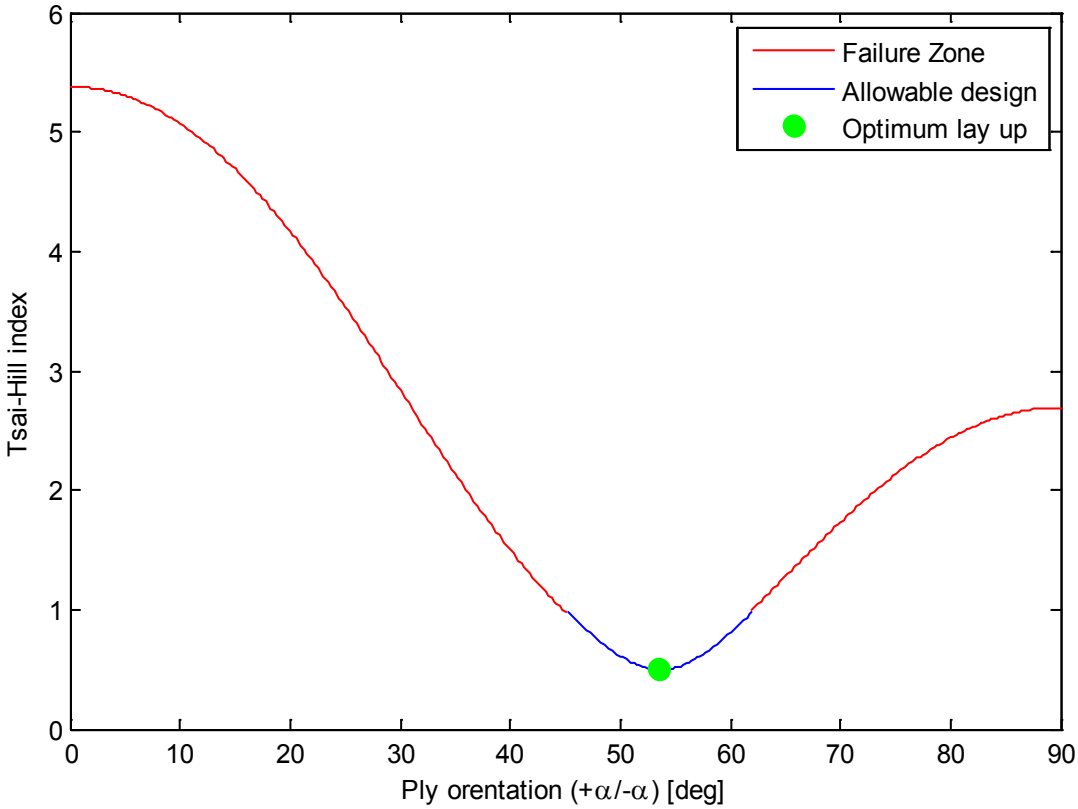

Figure 9. Tsai-Hill index distribution for the angle ply pressure vessel at different $(+\alpha/-\alpha)_{12S}$ orientations

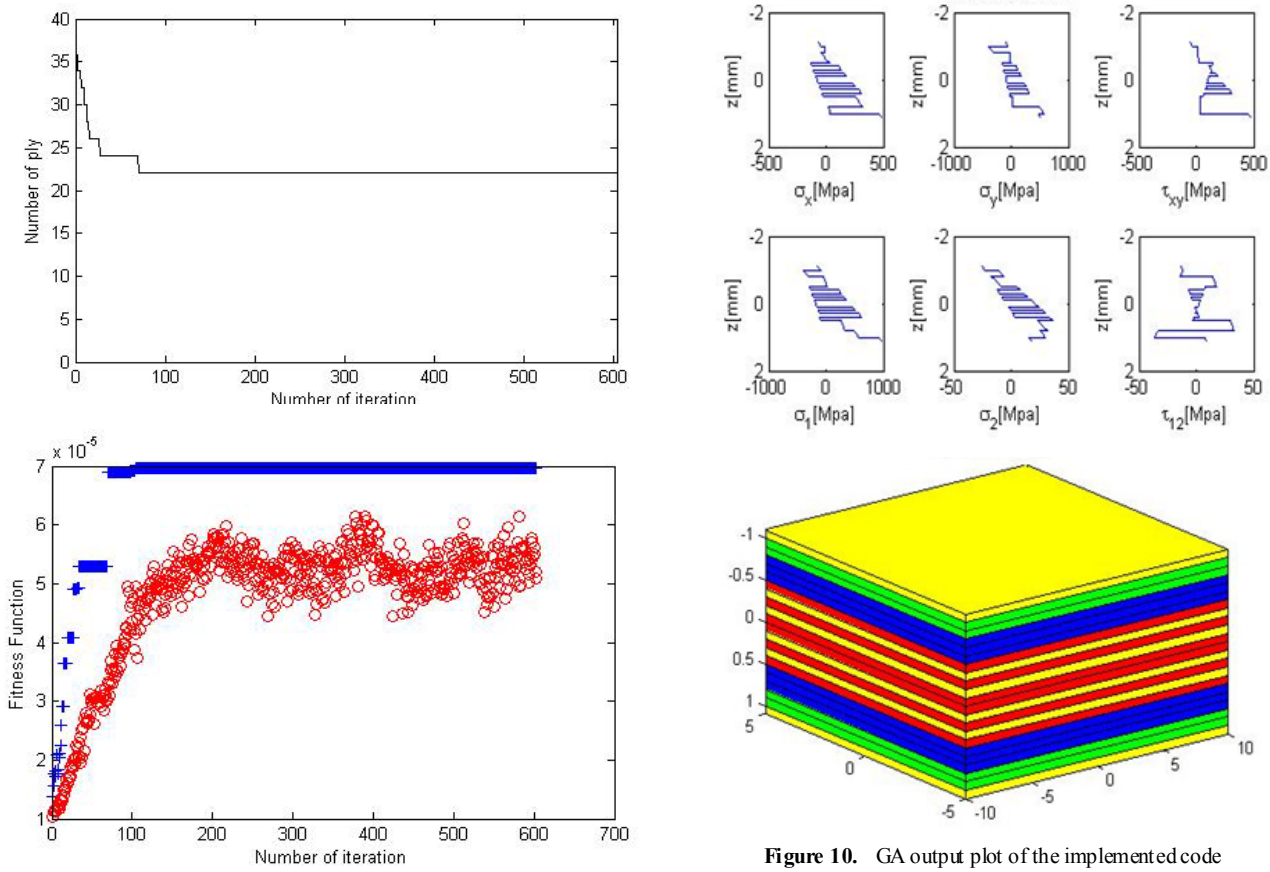

Figure 10. GA output plot of the implemented code

In this case, the burst pressure computed with (6.1) or (6.2) depends on whether FPF or LPF is used. Taking into account inertial loads implies a tank that is less efficient in pressure containment; the ratio between burst pressure and internal pressure is greater than two for the non-inertia case and less than 2 for the inertia case (considering FPF). The genetic algorithm output is shown in Figure 10. During the population evolution, using the subplot, the GA routine plots the value of the best laminate fitness (blue marker) in real time and the value of the mean fitness population (red circle). At the end of the evolution, the figure is completed by plotting the laminate layup and the state of stress in both geometric (x,y) and the orthotropic coordinate systems (1,2). The mean fitness value (red circle) is characterized by the oscillations that can be observed in figure 10, as it is the mean value of the whole population in which the fitness of the laminates that do not satisfy the failure criterion is forced to zero; i.e. the mean fitness value is evaluated as the sum of the fitness of each laminate of the i^{th} population divided by the size of the population.

Typical behaviour of the genetic algorithm was observed, although the presence of oscillations and convergence of the population to the best fitness were also observed.

6. Probabilistic Approachto the Pressure Vessel Composite Structure

The previously presented analysis was conducted to define the characteristics of the tank in order to focus on a specific configuration with respect to the performance index, regardless of which material is used to manufacture the tank. In the case of real applications, composite materials offer the possibility of improving the performance index manufacturing lightweight tanks. On the other hand, the safety/knockdown factors adopted for metals could be inadequate when innovative structural configurations and/or materials are considered. For example, if composite materials are adopted, traditional procedures lead to a "worst case" approach that is too penalizing to take into account their great dispersion and sensitivity to environmental conditions.

Moreover, when safety/knockdown factors are used, no quantitative information is obtained on the safety or reliability level of the structures and it is thus almost impossible to evaluate the impact of different structural options on the safety and reliability or to have a constant level of criticality in each structural component. Both of these drawbacks lead to an increment in the weight of the structure without an equivalent or known increment in structural safety.

A probabilistic approach is able to strengthen the understanding of the design process, since the designer has a measure of reliability and a safety level at his disposal during the process itself.

A probabilistic preliminary design methodology for composite structures, in which the safety level is guaranteed by means of a quantitative measure, such as the nominal probability of failure, was developed in[18] and is here summarized and applied for the case of a composite filament-wound pressure vessel. The procedure can be described briefly through the following steps:

1) Definition of a target probability of failure; definition of the initial structural configuration and description of the probabilistic interdependency of the structural components; definition of the sizing strategy;

2) evaluation of a first attempt "resistance effect" increment in order to meet the required probability of failure;

3) sizing of the structure in order to achieve the resistance level evaluated in 2;

4) evaluation of the probability of failure of the new structural configuration: if this does not meet the target probability, a new loop is started from point 2 trough to point 4. Instead, if the target probability is met, a refinement of the structure is performed in order to check whether the configuration obtained in 3 presents the minimum possible number of layers that can guarantee the target probability.

The model adopted for the pressure vessel is the one that was reported in[19]. The filament-wound pressure vessel is assumed to have adjacent ±θ angle layups that act as orthotropic units, as in Figure 11; the length of the vessel is considered large enough to consider the longitudinal bending due to the end closures as being limited to small portions of the tank itself, and longitudinal bending is therefore neglected.

This case can be treated as a generalized plane stress problem. The adopted failure prediction criterion for a single layer of the orthotropic layer ±θ was the 3D quadratic one reported in[15] :

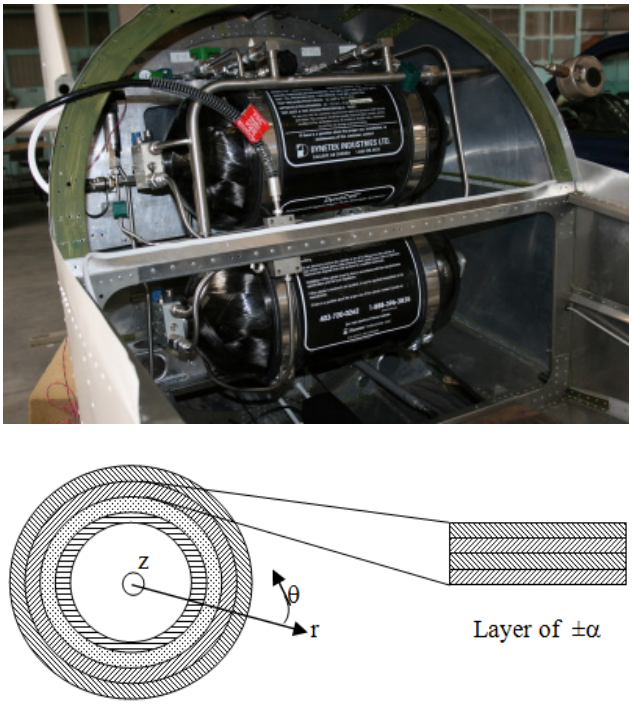

Figure 11. Cylindrical pressure vessel scheme

$$F_{zz}\sigma_z^2 + F_{rr}\left(\sigma_r^2 + \sigma_\vartheta^2\right) + F_{ss}\tau_{\vartheta z}^2 + 2F_{rz}\left(\sigma_r + \sigma_\vartheta\right)\sigma_z + 2F_{r\vartheta}\sigma_r\sigma_\vartheta + F_r\left(\sigma_r + \sigma_\vartheta\right) + F_z\sigma_z - 1 = 0 \quad (7)$$

where F represents the material strength in the direction indicated by the subscripts and relative to tension (*t*), and compression (*c*). The probabilistic sizing was performed considering the entire pressure vessel as a single component described by the limit state function G=*burst pressure* – applied pressure P; the burst pressure was the minimum pressure that can verifies the above.

The target probability of failure was chosen as 10^{-4}. The random variables considered in the analysis are reported in table 4. Since the adopted sizing strategy was to add or subtract an orthotropic unit without changing the winding angle, a preliminary parametric analysis of failure probability was performed as a function of α; a 20 layer pressure vessel was used for this investigation and as the starting structural configuration for the sizing procedure. As can be observed in fig. 12, the probability of failure presents a minimum of 57° , in accordance with the results generally obtained in the deterministic design of angles that optimize burst pressure. This angle was used for the probabilistic sizing. The sizing was performed for different values of the internal radius R_i in order to check the correct behaviour of the software; fewer layers can be expected for smaller radiuses.

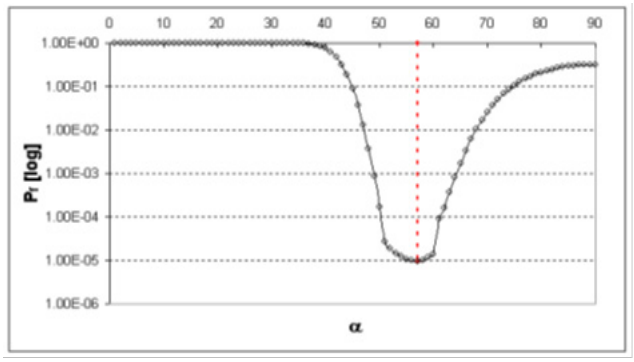

Figure 12. Probability of failure of a 20 layer pressure vessel against the winding angle[20]

Table 4. Probabilistic analysis - definition of the random variables

Nome Variabile	Distribuzione	Valore Atteso	Deviazione Standard	U.M.	n° Variabili
E_f	Weibull	213200	21581	MPa	1
E_m	Weibull	3459	350	MPa	1
G_f	Weibull	8960	906	MPa	1
G_m	Weibull	1293	131	MPa	1
$\%V_f$	Normale	0.6	0.06	-	1
ν_f	Normale	0.2	0.02	-	1
θ	Normale	0	1	°	1
Stot	Normale	0.712	0.1424	mm	1
S_{1t}	Weibull	1400	142	MPa	1
S_{1c}	Weibull	1255	127	MPa	1
S_{2t}	Weibull	105	11	MPa	1
S_{2c}	Weibull	240	24	MPa	1
S_{12}	Weibull	90	12	MPa	1

7. Conclusions

The optimization of a composite pressure vessel has been presented in the present work.

From the general sizing of the hydrogen tank, it has emerged that the configuration that satisfies the whole set of requirements is the one in which two tanks are necessary to store hydrogen at a pressure of 100 bar.

A progressive ply failure analysis code has been developed to compute the failure loads of a generic laminate subjected to mechanical loads. The PPFA code has been validated and it shows a good correlation between the experimental and the FE results. It has been shown that failure loads are necessary to calculate the burst pressure of the composite vessel and ensure fulfilment of regulation requirements.

A genetic algorithm has been developed to optimize the layup of the composite vessel in order to save mass and reduce the influence of inertial loads. The optimized layup obtained from the GA runs was remarkably different from the case in which inertial loads were taken into account. The optimized stack sequence has in fact shown a notable presence of almost 0° plies in order to ensure an appropriate bending stiffness.

An approach to the reliability based design of pressure vessels has also been presented in order to ensure a given probability of failure.

Nomenclature

a	= panel length along the x direction
A_{ij}	= membrane stiffness matrix coefficient
D	= tank diameter
E_f	= Young's modulus of the fibre
E_m	= Young's modulus of the matrix
FH	=Hydrogen flow rate
FL	= Failure Load
FPF	= First Ply Failure
G	= limit state function
GA	= Genetic Algorithm
G_f	= shear modulus of the fibre
G_m	= shear modulus of the matrix
h,S_{tot}	= total panel thickness
LPF	= Last Ply Failure
MH	= Hydrogen mass
M_x	= bending moment
n	= number of half-laminate plies
P	= applied pressure
p_{burst}	= burst pressure
PEM	= Polymer Electrolyte Membrane
P_O	= Power required
PPFA	= Progressive Ply Failure Analysis
$p_{storage}$,p_{ex}	= storage pressure, exercise pressure
PV	= Pressure Vessel
S_{12}	= failure stress in shear mode
s_i	= thickness of the i-th ply
S_{ic}	= failure stress in compression alongthei-thdirection
S_{it}	= failure stress in tension along the i-th direction
t	=operational time
UAV	= Unmanned Aerial Vehicle
V	= cell voltage

V_f	= volume fraction of fibres in percentage
x, y	= geometric coordinate system
1,2	= orthotropic coordinate system
α	= ply orientation for angle ply laminate $\pm\alpha$
$\Delta N_{x,FPF,LPF}$	= load increment along the x direction until FPF or LPF
$\Delta N_{y\ FPF,LPF}$	= load increment along the y direction until FPF or LPF
Δp	= pressure increment
η_{FC}	= Fuel cell efficiency
θ	= ply orientation
σ_i	= membrane stress induced in the i-th ply by the bending moment

REFERENCES

[1] Romeo G.: "Design Proposal of High Altitude Very-Long Endurance Solar Powered Platform for Earth Observation and Telecommunication Applications". 48th Int. Astronautical Congress (IAF), October 6-10, 1997, Turin. Paper n. IAF-97-M.2.05.

[2] Romeo G.: "Design of High Altitude Very-Long Endurance Solar-Powered Platform for Earth Observation and Telecommunication Applications".Journal Aerotecnica Missili e Spazio,Vol.77, N.3-4, July-Dec.98. pp. 88-99.

[3] Romeo G., Frulla G., Cestino E., Corsino G.: "HELIPLAT: Design, Aerodynamic Structural Analysis of Long - Endurance Solar-Powered Stratospheric Platform".AIAA Journal of Aircraft, Vol. 41, No. 6, Nov-Dic 2004, pp. 1505-1520. (ISSN: 0021-8669)

[4] Romeo G., Frulla G.: "HELIPLAT: High Altitude Very-Long Endurance Solar Powered UAV for Telecommunication and Earth Observation Applications".The Aeronautical Journal. Vol.108, N.1084, June 2004, pp. 277-293. (ISSN: 0001-9240)

[5] Romeo G., Frulla G.: "HELIPLAT: Aerodynamic and Structural Analysis of HAVE Solar Powered Platform". 1st AIAA Technical Conference & Workshop on Unmanned Aerospace Vehicles, Systems, Technologies & Operations. Portsmouth, VA, USA, 20-23 May 2002. ISBN: 1-56347-565-0

[6] Romeo G., Frulla G., Fattore L.: "HELIPLAT: High Altitude Very-Long Endurance Solar Powered UAV for Telecommunication Applications. FEM Analysis, Manufacturing and Testing of 21m long CFRP Wing Box".. Applied Vehicle Technology Panel Symposium on Unmanned Vehicles (UV) for Aerial, Ground and Naval Military Operations. Ankara (Turkey) Oct. 2000. RTO Meeting Proc.: MP-052, Paper N.12.

[7] Romeo G.,Frulla G., Cestino E., Marzocca P.:" Non-linear Aeroelastic Behavior of Highly Flexible HALE Wings". 25thInternational Congress of the Aeronautical Sciences (ICAS 2006), 3-8 September 2006, Hamburg, Germany, 11pages. ISBN: 0-9533991-7-6.

[8] Tuzcu I., Marzocca P., Cestino E., Romeo G., Frulla G.,: "Stability and Control of a High - Altitude-Long-Endura nce UAV", Journal of Guidance, Control, and Dynamics, Vol.30, No.3, May-June 2007, pp.713-721. (ISSN: 0731-5090)

[9] Romeo G., Frulla G., Cestino E. "Design of high altitude long endurance solar powered unmanned air vehicle for multi-payload and operations", Proc. of the Institution of Mechanical Engineers. Part G, Journal of Aerospace Engineering, Vol.221, 2007, pp.199-216. (ISSN: 0954-4100). DOI: 10.1243/09544100JAERO119.

[10] Romeo G; Borello F: "Very-Long Endurance Solar Powered Autonomous Stratospheric UAV For Mediterranean Sea Border Surveillance, Forest Fire Monitoring, Fishery". 33th International Symposium on Remote Sensing of Environment (33 ISRSE). JRC, Stresa, Italy, 4-9 May 2009. Paper n. 656.

[11] Romeo G., Cestino E., Borello F., Pacino M.: "Very-Long Endurance Solar Powered Autonomous UAVS: Role and Constrants for GMES Applications".28th Int. Conf. of the Aeronautical Sciences (ICAS 2012), Brisbane (Australia), 23-28 Sept. 2012. Paper ID294.

[12] Romeo G., Borello F., Correa G.: "Set-Up and Test Flights of an All-Electric Aeroplane Powered by Fuel Cells",AIAA Journal of Aircraft, 2011, Vol. 49, N.4 (July-Aug. 2011), pp.1331-1341. DOI: 10.2514/1.55329.

[13] Colozza A. J., "Hydrogen Storage for Aircraft Applications Overview", NASA/CR—211867, 2002

[14] W. Xiangyang, C. Jianqiao, "Robust optimum of laminated composite plates", Acta Mechanics SolidaSinica, Vol 17, No. 4, December, 2004

[15] TsaiS.W.,"Composite design. Think Composites", Dayton, Oh, 1988.

[16] S. Tolson, N. Zabaras, "Finite element analysis ofprogressive failure in laminated composite plates", Composite and Structure Vol. 38, No 3,pp. 361-376, 1991.

[17] S.R. Soni, "A new look at commonly used failure theories in composite laminate", 24th AIAA/ASME/AHS Structures, Structural Dynamics and Materials Conference, Procedures, pp.171-179, 1983

[18] Borello F., "Approccio probabilistico al progetto di strutture aeronautiche in materiali compositi avanzati". PhD. Thesis. Politecnico di Torino, 2008

[19] Lekhnitskii S.G.,"Theory of Elasticity of an anisotropic elastic body."Holden-Day Inc: San Francisco, Ca, 1963.

[20] G.Frulla, F. Borello, "Structural reliability aspects for advanced composite material applications". in Reliability Engineering Advances, Nova publisher 2009 ISBN 978-1-60692-329-0.

[21] Frulla G; Cestino E.; Marzocca P, "Critical Behaviour of Slender Wing Configurations". Proc. of the Institution of Mechanical Engineers. Part G, Journal of Aerospace Engineering, vol. 224, pp. 587-600

[22] Noll T.E. etal., "Investigation of the Helios Prototype Aircraft Mishap" Volume I - NASA Mishap report, Jan. 2004.

[23] Romeo G., Frulla G., Cestino E., "Design of high-altitude long-endurance solar-powered unmanned air vehicle for multi-payload and operations". In: Proceedings of The Institution Of Mechanical Engineers. Part G, Journal of Aerospace Engineering, vol. 221, pp. 199-216.

[24] Mitchell M., "An introduction to Genetic Algorithm", A Bradford Book, The MIT Press Cambridge, Massachusetts, London, England Fifth printing, 1999.